Electric field suppression of ultracold confined chemical reactions

Goulven Quéméner and John L. Bohn

JILA, NIST and University of Colorado, Boulder, Colorado 80309-0440, USA

We consider ultracold collisions of polar molecules confined in a one-dimensional optical lattice. Using a quantum scattering formalism and a frame transformation method, we calculate elastic and chemical quenching rate constants for fermionic molecules. Taking ^{40}K^{87}Rb molecules as a prototype, we find that the rate of quenching collisions is *enhanced* at zero electric field as the confinement is increased but that this rate is *suppressed* when the electric field is turned on. For molecules with 500 nK of collision energy, for realistic molecular densities, and for achievable experimental electric fields and trap confinements, we predict lifetimes for KRb molecules to be 1 s. We find a ratio of elastic to quenching collision rates of about 100, which may be sufficient to achieve efficient evaporative cooling of polar KRb molecules.

PACS number(s): 34.50.Cx, 34.50.Lf

The recent achievement of ultracold polar molecules [1–3] has opened tremendous possibilities for the ultracold community. Individual quantum states of the molecules can now be addressed experimentally [2,4]. Beyond the idea of creating molecular Bose-Einstein condensates or degenerate Fermi gases of polar molecules, these "quantum-state-controlled" molecules have applications in ultracold chemistry [5,6], condensed matter and many-body physics [7,8], quantum information [9,10], and precision measurement and tests of fundamental laws [11]. These applications crucially depend on the collisional properties of the polar molecules in the presence of an electric field. To get a stable gas of molecules, elastic processes should dominate over quenching (including inelastic and/or reactive) processes. This is the case for molecules for which chemical reactions are energetically forbidden in their absolute ground state. For others, such as KRb molecules, chemical reactions such as KRb + KRb → K$_2$ + Rb$_2$ are energetically allowed [5,12,13], and evaporative cooling might be difficult to achieve. Chemical rates increase to the sixth power of the dipole moment induced by an electric field, due to head-to-tail collisions of the polar molecules [14,15]. On the other hand, these collisions may be suppressed in a one-dimensional (1D) optical lattice [8,16] that confines the molecules in planes perpendicular to the axis of their polarization so that the dipoles mutually repel each other.

In this article, we describe ultracold collisions of polar molecules in an electric field confined in a 1D optical lattice. We apply the theory to predict the elastic and chemical rate of confined KRb + KRb → K$_2$ + Rb$_2$ reactions to which particular attention is devoted [2,4,5,14] and for which theoretical predictions are needed. We show that the electric field suppression of confined chemical rates can help to achieve efficient evaporative cooling of such molecules. We assume that the wells of the 1D optical lattice are deep enough so that the molecules cannot tunnel from site to site and can be approximated by independent harmonic oscillator traps. In the following, quantities are expressed in SI units, unless explicitly stated otherwise. Atomic units (a.u.) are obtained by setting $\hbar = 4\pi\varepsilon_0 = 1$.

We consider pairs of bosonic or fermionic polar molecules of mass m and reduced mass $\mu = m/2$ confined in a har-

monic oscillator trapping potential $V_{\text{ho}} = \mu\omega^2 z^2/2$, which allows the molecules to collide in a two-dimensional (2D) configuration space. The electric field is applied along the z direction, perpendicular to the planes of free motion in the trap. The Hamiltonian in the relative coordinate $\vec{R}$ is given by

$$H = -\frac{\hbar^2}{2\mu}\nabla^2 + V_{\text{ho}} + V_{\text{vdW}} + V_{\text{dd}} + V_{\text{abs}}. \tag{1}$$

The long-range interactions are represented by the van der Waals potential $V_{\text{vdW}} = -C_6/R^6$, and the dipole-dipole interaction $V_{\text{dd}} = d^2(1 - 3\cos^2\theta)/(4\pi\varepsilon_0 R^3)$, where d represents the effective dipole moment of the polar molecule induced by the electric field [15]. Moreover, we represent chemical reactions via the non-Hermitian, absorbing potential $V_{\text{abs}} = iAe^{-(R-R_0)/R_c}$, with $A = 10$ K, $R_0 = 10\ a_0$, and $R_c = 10\ a_0$ (a_0 is the Bohr radius), which has been chosen to successfully describe three-dimensional (3D) chemical rates of KRb molecules in an electric field, measured in Ref. [14].

Scattering wave functions Ψ are most naturally described at large intermolecular spacing in cylindrical coordinates $\vec{R} = (\rho, z, \varphi)$ in accordance with the symmetry of the confined trapping potential. The interactions between molecules when they are closer together, however, are better described in spherical coordinates $\vec{R} = (R, \theta, \varphi)$. In our numerical calculations, we therefore use the appropriate coordinate system and then weld the wave functions together at a suitable matching distance. Note that the azimuthal angle φ is common to both coordinate systems, and in fact the Hamiltonian is independent of φ. Therefore, the quantum number M, representing the azimuthal projection of the orbital angular momentum, is rigorously conserved. Note also that in the limit of strong confinement, θ is restricted to values near $\theta \approx \pi/2$, in which case the dipolar interaction is repulsive. This is the primary principle behind the electric field suppression of collisions.

When the molecules are close together, we solve the coupled-channel equations of motion in spherical coordinates using the diabatic-by-sector method [17]. We divide the complete range of R into sectors labeled by an index p. In

each sector, we expand the M-dependent wave function of an initial channel i as

$$\Psi_i^M(R,\theta) = \frac{1}{R} \sum_j \chi_j^M(R_p;\theta) F_{ji}^M(R_p;R). \quad (2)$$

The adiabatic functions $\chi_j^M(R_p;\theta)$ are those that diagonalize the M-dependent angular part $\mathcal{H}^M(R,\theta)$ of the Hamiltonian in Eq. (1) at the fixed radius $R = R_p$, the middle of the sector p. The associated adiabatic energy is $\epsilon_j(R_p)$, which converges to a harmonic oscillator energy ε_n of a state n of the trap at large R_p. The radial functions $F_{fi}^M(R_p;R)$, where $f = 1,2,\ldots$ represents an arbitrary final channel of the system, are determined within each sector according to the diabatic equations of motion

$$\left(-\frac{\hbar^2}{2\mu}\frac{d^2}{dR^2} - E\right) F_{fi}^M(R_p;R) + \sum_j \mathcal{U}_{fj}^M(R_p;R)\, F_{ji}^M(R_p;R)$$
$$= 0, \quad (3)$$

where

$$\mathcal{U}_{fj}^M(R_p;R) = \int_0^\pi \chi_f^M(R_p;\theta)\mathcal{H}^M(R,\theta)\chi_j^M(R_p;\theta)\sin\theta d\theta. \quad (4)$$

E is the total energy of the system. To solve Eq. (3), we employ the method of the propagation of the logarithmic derivative matrix $Z^M = (F^M)'(F^M)^{-1}$ of Johnson [18] up to a suitable matching radius R_m.

If R_m is sufficiently large, then the only potential energy of any significance is the trap confinement potential V_{ho}. At this point, the wave function is more conveniently described in cylindrical coordinates. Therefore, for an initial state n_i of the trap, we expand the M-dependent wave function as

$$\Psi_{n_i}^M(\rho,z) = \frac{1}{\rho^{1/2}} \sum_{n_f} g_{n_f}(z) G_{n_f n_i}^M(\rho), \quad (5)$$

where $g_{n_f}(z)$ are normalized harmonic oscillator functions in z corresponding to a state n_f of the trap. We checked that the functions $\rho^{1/2}\chi_f^M/R$ converged to the $g_{n_f}(z)$ functions at large R_m. The radial functions G^M serve to define the reactance matrix K^M via $G_{n_f n_i}^M(\rho) \propto \rho^{1/2} J_M(k_{n_f}\rho)\delta_{n_f n_i} + \rho^{1/2}N_M(k_{n_f}\rho)K_{n_f n_i}^M$, in terms of Bessel functions J_M, N_M. For closed channels, modified Bessel functions must to be used instead; $k_{n_f} = \sqrt{2\mu(E - \varepsilon_{n_f})}/\hbar$ represents the wave vector of the relative motion of the state n_f. For the initial oscillator state n_i, $k_{n_i} = \sqrt{2\mu E_c}/\hbar$, where $E_c = E - \varepsilon_{n_i}$ is the initial collision energy. The K^M matrix is found by a matching procedure from the spherical wave function that captures the short-range physics and the cylindrical wave function that captures the asymptotic boundary conditions. This is done by equating Eq. (2) to Eq. (5) along with their radial derivatives, at a constant radius $R = R_m$ [17]. The matching procedure yields two regular and irregular spherical radial functions and derivatives. The accuracy of the procedure is checked by their Wronskian matrix, which converges at large R_m to a diagonal unit matrix.

The K^M matrix in turn determines the scattering matrix $S^M = (I + iK^M)^{-1}(I - iK^M)$, where I represents a diagonal unit matrix. The cross sections for elastic and quenching collisions are given by [19–21]

$$\sigma^{\text{el}} = \frac{\hbar}{\sqrt{2\mu E_c}} \sum_M \left|1 - S_{n_i n_i}^M\right|^2 \Delta, \quad (6)$$

$$\sigma^{\text{qu}} = \frac{\hbar}{\sqrt{2\mu E_c}} \sum_M \left(1 - \left|S_{n_i n_i}^M\right|^2\right)\Delta, \quad (7)$$

and the rate coefficient is given by $\mathcal{K}^{\text{el,qu}} = \sigma^{\text{el,qu}} \times v$, where $v = \sqrt{2E_c/\mu}$ is the collision velocity. The factor Δ represents symmetrization requirements for identical particles: $\Delta = 1,2$, accordingly, as the particles are distinguishable or indistinguishable. To compare with experimental results, one should average the rate coefficients over a Maxwell-Boltzmann distribution of the velocity v, but we do not perform this average here. Finally, due to exchange symmetry of indistinguishable molecules, the quantum numbers in the asymptotic representation Eq. (5) satisfy the relation

$$(-1)^{n+M} = \gamma, \quad (8)$$

with $\gamma = +1$ for bosonic molecules and $\gamma = -1$ for fermionic molecules.

For concreteness, we now consider collisions of fermionic $^{40}\text{K}^{87}\text{Rb}$ molecules, prepared in same internal states. We use the actual mass and permanent dipole moment of these molecules, and set the coefficient of their van der Waals interaction to $C_6 = 21\,000$ a.u. [14] (1 a.u. $= 1\ E_h a_0^6$, where E_h is the Hartree energy). We consider only pairs of molecules initially confined to the ground state of the harmonic oscillator, with $n_i = n_f = 0$, and we take the collision energy to be $E_c = 500$ nK, relevant in the ongoing KRb experiment. Under these circumstances, we find converged results at a matching radius $R_m = 10^4 a_0$. As the pairs of fermionic molecules are in the ground harmonic oscillator state $n = 0$, only odd values of M are allowed in Eq. (8). This circumstance removes the occurrence of undesired head-to-tail collisions ($M = 0$) of the molecules in an electric field at ultralow collision energy. At $E_c = 500$ nK, we find that scattering is largely dominated by the single partial wave $M = 1$. Despite the fact that the molecules are in the ground state of the trap, we need to employ one open channel ($n = 0$) and three closed channels ($n = 2,4,6$) to converge the results to 10%.

The characteristic lengths (a) and energies (E) of the different interactions involved in the chemical process are presented in Table I. They are given for the various interactions

TABLE I. Characteristic lengths and energies of the different interactions involved in the KRb + KRb collision; 1 D = 1 Debye = $3.336\,10^{-30}$ C m.

Interaction	$a_{\text{vdW,dd,ho}}$ (units of a_0)	$E_{\text{vdw,dd,ho}}$ (μK)
$C_6 = 21\,000$ a.u.	264	19.6
$d = 0.1$ D	179	85.2
$d = 0.2$ D	716	5.3
$d = 0.3$ D	1611	1.06
$d = 0.566$ D	5734	0.083
$\nu = 50$ kHz	1069	2.4
$\nu = 100$ kHz	239	48

by $a_{vdW} = (2\mu C_6/\hbar^2)^{1/4}$ and $E_{vdW} = \hbar^2/(2\mu a_{vdW}^2)$ for the van der Waals interaction, $a_{dd}(d) = \mu d^2/\hbar^2$ and $E_{dd}(d) = \hbar^6/(\mu^3 d^4)$ for the dipole-dipole interaction, and $a_{ho}(\nu) = \sqrt{\hbar/(2\pi\nu\mu)} = \sqrt{\hbar/(\omega\mu)}$ and $E_{ho}(\nu) = \hbar 2\pi\nu = \hbar\omega$ for the harmonic oscillator trap. This is useful for characterizing the different regimes involved in the chemical process. When a_{vdW} or $a_{dd} < a_{ho}$, intermolecular forces take place where the confinement is small and the collisions are effectively 3D. When $a_{ho} < a_{vdW}$ or a_{dd}, the reverse is true and the collisions are effectively 2D. For fermions in $n = 0$ and when an electric field is applied, the molecules meet primarily side by side and repel each other. For weakly polarized molecules, trap frequencies of 50 kHz and 1000 kHz are representative of the 3D and 2D limits, respectively (see Table I). For more strongly polarized molecules at $d > 0.3$ D, the 2D limit is reached for both confinements as $a_{ho} < a_{dd}$. We consider the two confinements in the following. We note that the present theoretical formalism can treat both 3D and 2D limits in an electric field. This is in contrast with former theoretical studies [22,23], which do not take into account the electric field and do not describe the 2D limit where $a_{ho} < a_{vdW}$ or a_{dd}.

We present in Fig. 1 the elastic and quenching rate coefficient as a function of the induced dipole moment d, for a trap frequency of $\nu = 50$ kHz (upper panel) and $\nu = 1000$ kHz (lower panel). The elastic rates (blue lines) have the same
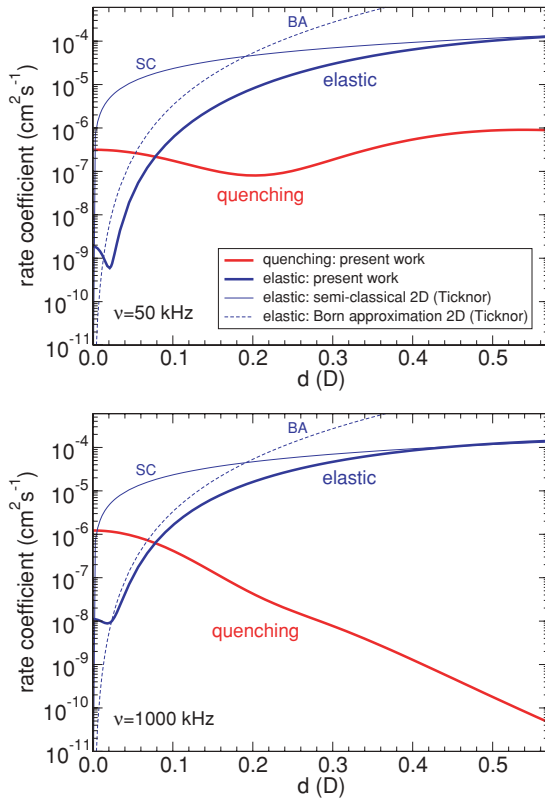

FIG. 1. (Color online) Collision of $^{40}K^{87}Rb$ molecules in the ground state of a confining trap. The elastic (blue) and quenching (red) rate coefficients are plotted as a function of the dipole moment d for $\nu = 50$ kHz (upper panel) and $\nu = 1000$ kHz (lower panel), for a fixed collision energy of $E_c = 500$ nK. A pure 2D SC formula (thin blue line) and a pure 2D Born approximation (BA) formula (dashed blue line) have also been reported from Ticknor [24].

trend for the two different confinements, increasing with the dipole moment. For $d > 0.2$ D, the elastic rates converge to a semiclassical (SC) formulation (thin blue lines) of pure 2D dipolar scattering [24], which increases linearly with d. For $d < 0.2$ D, the elastic rates are in better agreement with a pure 2D Born approximation (BA; dashed blue lines) that scales as d^4 [24]. For $d \simeq 0$ D, the elastic rates take a finite value, which is determined by an unknown scattering phase shift which depends on the short-range potential of KRb–KRb. We note that the overall elastic rate is in better agreement with the pure 2D estimations for the larger confinement $\nu = 1000$ kHz than for the smaller confinement $\nu = 50$ kHz, as one expects.

In contrast, the quenching rates (red lines) have a different trend with dipole moment for the two different confinement strengths. For $\nu = 50$ kHz (upper panel), the quenching rate first decreases and then increases again as a function of d. This behavior already contrasts with the quenching rate in 3D collisions, which increases as d^6 in the absence of z confinement [14,15]. The crucial difference comes from the fact that destructive head-to-tail collisions ($M = 0$) are removed by the confined geometry for fermions in the ground state $n = 0$ [see Eq. (8)]. Under even greater confinement (lower panel), the quenching rate continues to decrease with increasing dipole moment [15,25], illustrating the electric field suppression of confined chemical rates.

To better understand the qualitative trend of the quenching rates, we present in Fig. 2 the height V_b of the effective potential energy barrier (see Ref. [15]) corresponding to the lowest adiabatic energy curve $\epsilon_{f=1}(R_p)$, as a function of d for $\nu = 50, 1000$ kHz. We follow the qualitative arguments given in Ref. [15] that the behavior of the quenching rates are suppressed by the need for the molecules to tunnel through this barrier to the region of chemical reactivity. For $\nu = 50$ kHz, the barrier increases for small dipole moments, since the dipole interaction is repulsive for $M = 1$. However, anisotropy of the interaction couples different channels together. Therefore, at higher dipole moments, the lowest adiabatic curve is repelled more strongly from the others, ultimately lowering the barrier height and increasing the quenching rate. For the stronger confinement $\nu = 1000$ kHz, the barrier height continues to grow as the dipole moment increases, leading to continued suppression of quenching by four orders of magnitude over the range of dipole moment shown. There are two ways
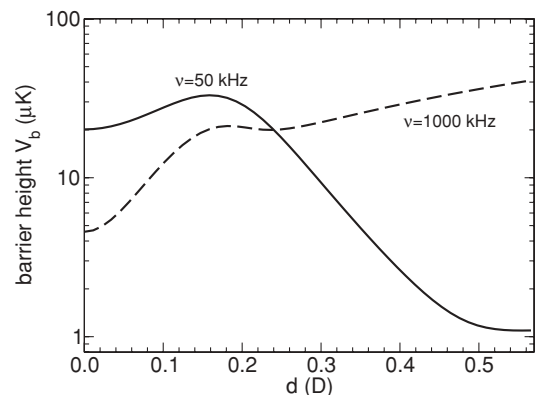

FIG. 2. Barrier height V_b as a function of the dipole moment d for $\nu = 50$ kHz (solid line) and $\nu = 1000$ kHz (dashed line).

to see this ongoing suppression of quenching. First, since $a_{ho}(1000 \text{ kHz}) < a_{vdW}$ or a_{dd}, the molecules exert strong dipolar forces on each other at long range where they are still described by harmonic oscillator states. Thus, the interaction remains overwhelmingly repulsive and the molecules do not get close enough to react. Alternatively, we note that the trap confinement is tight enough so that the spacing between the harmonic trap levels is large, and therefore the repulsion between adiabatic channels is small. The incident adiabatic channel is therefore less likely to be lowered due to the presence of other locally open adiabatic channels at short range. As a result, the barrier height continues to increase as d increases, driven solely by the increasing dipolar repulsion.

The calculations show another interesting trend as confinement is increased. Namely, at zero dipole moment, the quenching rate is higher for the tighter confinement $\nu = 1000$ kHz. This is consistent with the barrier height V_b being smaller for the higher trap frequency (Fig. 2). This difference arises from the fact that the collision energy is measured relative to the asymptotic energy of the potential, which is the zero-point energy of the confining potential. The tighter trap has a higher zero-point energy (Table I), and hence the apparent barrier is lower.

Finally, Fig. 1 shows that for an experimentally achievable frequency trap of $\nu = 50$ kHz (upper panel), we predict a loss rate of $\sim 10^{-7}$ cm^2 s^{-1} per molecule for the maximum dipole moment $d = 0.2$ D achieved so far in the KRb experiment. For a realistic planar density of molecules $\sim 10^7$ cm^{-2}, this corresponds to molecular lifetimes of ~ 1 s, which is 100 times longer than if the molecules were not confined. Equally important is the ratio of elastic to quenching collisions. At $d = 0.2$ D for $\nu = 50$ kHz, we predict ~ 100 elastic collisions before a chemical reaction occurs. This ratio may be sufficiently high to achieve efficient evaporative cooling of KRb molecules in a 1D optical lattice and to pave the way for a long-lived quantum gas of polar molecules.

Note added in proofs. We have been aware of a complementary study which can be found in Ref. [26].

[1] J. M. Sage, S. Sainis, T. Bergeman, and D. DeMille, Phys. Rev. Lett. **94**, 203001 (2005).

[2] K.-K. Ni *et al.*, Science **322**, 231 (2008).

[3] J. Deiglmayr *et al.*, Phys. Rev. Lett. **101**, 133004 (2008).

[4] S. Ospelkaus *et al.*, Phys. Rev. Lett. **104**, 030402 (2010).

[5] S. Ospelkaus *et al.*, Science **327**, 853 (2010).

[6] R. V. Krems, Phys. Chem. Chem. Phys. **10**, 4079 (2008).

[7] A. Micheli, G. K. Brennen, and P. Zoller, Nat. Phys. **2**, 341 (2006).

[8] H. P. Büchler *et al.*, Phys. Rev. Lett. **98**, 060404 (2007).

[9] D. DeMille, Phys. Rev. Lett. **88**, 067901 (2002).

[10] S. F. Yelin, K. Kirby, and R. Côté, Phys. Rev. A **74**, 050301(R) (2006).

[11] L. D. Carr *et al.*, New J. Phys. **11**, 055049 (2009).

[12] P. S. Żuchowski and J. M. Hutson, e-print arXiv:1003.1418.

[13] E. R. Meyer and J. L. Bohn, e-print arXiv:1004.3317.

[14] K.-K. Ni *et al.*, Nature **464**, 1324 (2010).

[15] G. Quéméner and J. L. Bohn, Phys. Rev. A **81**, 022702 (2010).

[16] A. Micheli, G. Pupillo, H. P. Buchler, and P. Zoller, Phys. Rev. A **76**, 043604 (2007).

[17] R. T. Pack and G. A. Parker, J. Chem. Phys. **87**, 3888 (1987).

[18] B. R. Johnson, J. Comput. Phys. **13**, 445 (1973).

[19] I. R. Lapidus, Am. J. Phys. **50**, 45 (1982).

[20] S. K. Adhikari, Am. J. Phys. **54**, 362 (1986).

[21] P. Naidon and P. S. Julienne, Phys. Rev. A **74**, 062713 (2006).

[22] D. S. Petrov and G. V. Shlyapnikov, Phys. Rev. A **64**, 012706 (2001).

[23] Z. Li and R. V. Krems, Phys. Rev. A **79**, 050701(R) (2009).

[24] C. Ticknor, Phys. Rev. A **80**, 052702 (2009).

[25] C. Ticknor, Phys. Rev. A **81**, 042708 (2010).

[26] A. Micheli, Z. Idziaszek, G. Pupillo, M. A. Baranov, P. Zoller, and P. S. Julienne, e-print arXiv:1004.5420.